

## DIAGNOSTICS OF HIGH FREQUENCY UNDERWATER DISCHARGES IN WATER SOLUTIONS BY ELECTRIC MEASUREMENTS

Kozáková Z., Vašíček M., Hlochová L., Krčma F.

*Brno University of Technology, Faculty of Chemistry, Purkyňova 464/118, 612 00 Brno, Czech Republic,  
[kozakova@fch.vutbr.cz](mailto:kozakova@fch.vutbr.cz)*

**Abstract:** This paper deals with electric discharges generated by high frequency high voltage (15–100 kHz) in NaCl solutions (conductivity of  $500 \mu\text{S}\cdot\text{cm}^{-1}$ ). A batch plasma reactor in the pin-hole configuration contained a ceramic dielectric barrier separating two planar stainless steel electrodes; barrier thickness of 0.6 mm, pin-hole diameter of 0.3 or 0.6 mm. Electrical measurements were employed in order to characterise energy dissipation during the discharge ignition. Lissajouse charts were evaluated for different discharge phases (electrolysis, bubble formation and discharge regular operation). Subsequently, discharge power was estimated from the charts and plotted as a function of applied frequency.

**Keywords:** underwater discharge, pin-hole discharge ignition, high frequency discharge, electrical measurements, Lissajouse charts, discharge power

### Introduction

Electrical discharges generated directly in liquids or as plasma in the direct interaction with the liquid phase are one of the hot topics of the contemporary plasma research. These systems can be applied for example in water treatment [1, 2], sterilization [3], and surface treatment of various temperature sensitive materials [4] as well as for the nanoparticles production [5]. The plasma in water solutions can be generated by various electrode configurations, and it can be supplied by many kinds of applied voltage from DC up to RF frequencies using pulsed as well as non-pulsed regimes.

The pin-hole discharge is one of suitable configurations allowing electrical discharge generation in liquids. Typically, DC or low frequency (50 Hz) high voltage sources are used in a pulsed or continuous regime [6]. Two of initiated processes, electrolysis and Joule heating, induce a decrease of energy efficiency of such systems [7]. Moreover, the applicability of such power supplies seems to be rather dangerous for handy operating devices. Thus, we have focused on the pin-hole discharge generation using an audio frequency power supply.

For plasma diagnostics of the pin-hole discharge, electrical measurements of the main electric values (discharge current, voltage, power and frequency) as well as other important additional parameters (light emission and sound records) were employed in order to determine particular processes during the discharge ignition in water solution.

### Experimental set-up

A batch discharge reactor with total volume of 100 ml was divided by a dielectric barrier into two electrode parts. The dielectric barrier was made of 0.6 mm thick Shapal-M<sup>TM</sup> ceramics with one central pin-hole with the diameter of 0.3 or 0.6 mm. One planar electrode ( $48\times 40 \text{ mm}^2$ ) made of stainless steel was installed in each part of the reactor in the distance of 45 mm from the dielectric barrier. NaCl solutions with initial conductivity of  $500 \mu\text{S}\cdot\text{cm}^{-1}$  were used as a conductive liquid in the presented study.

A specially designed power supply based on a resonance circuit gave sinusoidal high voltage up to 5 kV. Its energy was set using frequency in the range of 15–100 kHz. The supplied energy was calculated using Lissajouse charts [8]. A four-channel oscilloscope Tektronix TDS 2024B was used for instantaneous records of voltage, current, light and sound before, during and after the discharge ignition. High voltage was measured by a Tektronix P6005A probe, current was determined from

voltage measured on a 4  $\mu\text{F}$  capacitor. A simplified scheme of the plasma reactor and its integration into the circuit with the power supply and the oscilloscope is given by Figure 1.

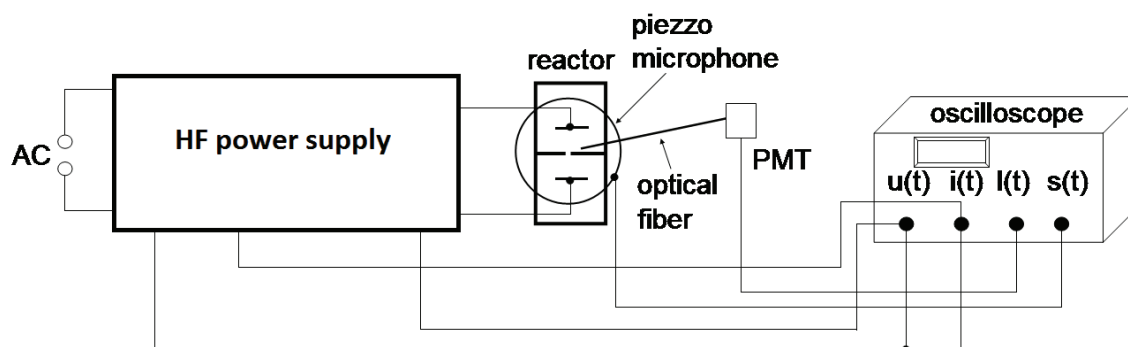


Figure 1. Simplified scheme of the pin-hole plasma reactor and its integration into the circuit with the high frequency HV source and the four-channel oscilloscope:  $u(t)$  – voltage,  $i(t)$  – current,  $l(t)$  – light,  $s(t)$  – sound.

## Results

Instantaneous values of current and voltage were recorded in several steps with the increasing applied voltage. Records of sound and emitted light were also observed in order to estimate bubble formation and discharge breakdown in the plasma reactor. Subsequently, Lissajouse charts [8] were constructed from data combining high voltage amplitude and voltage measured on the capacitor (4.142  $\mu\text{F}$ ). Final Lissajouse charts for four different phases during the pin-hole discharge ignition are presented in Figure 2.

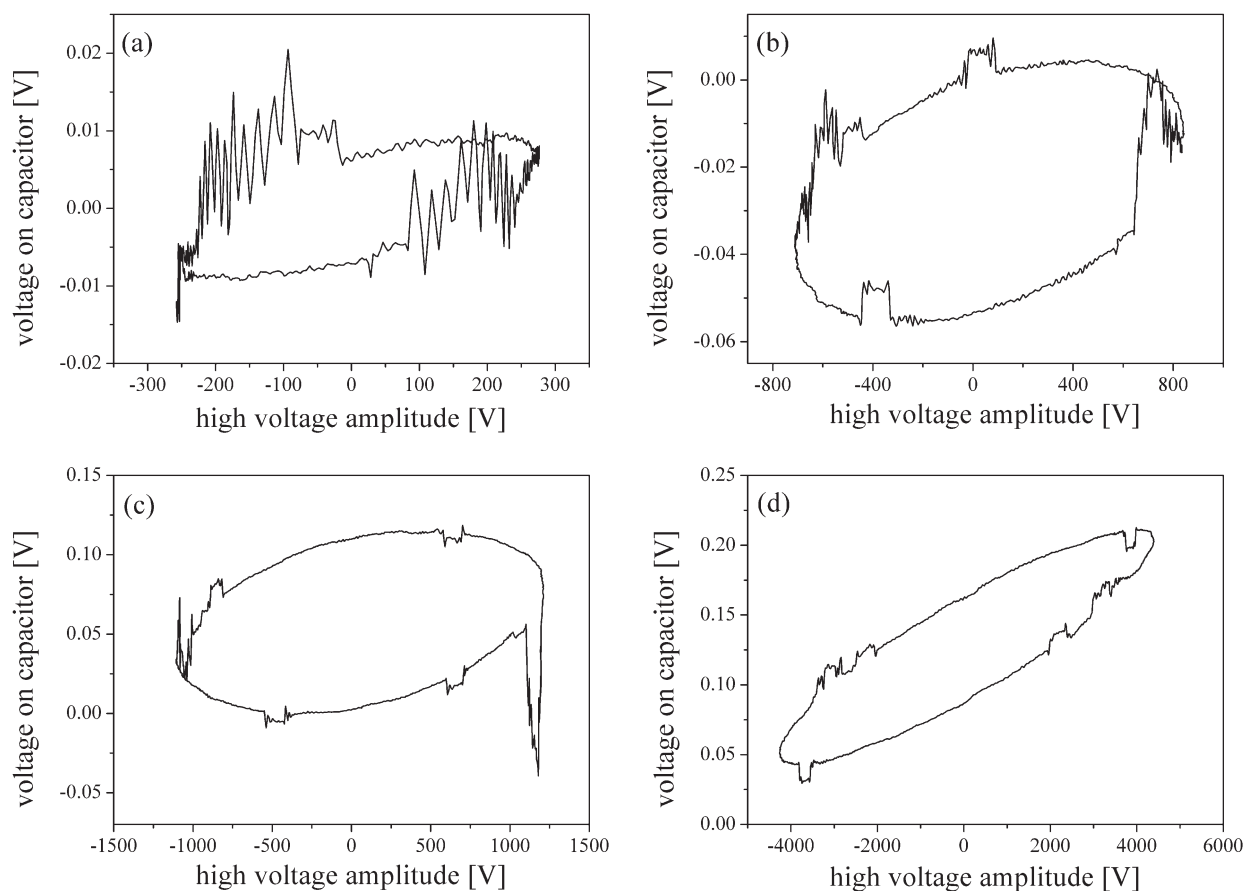


Figure 2. Lissajouse charts for four processes occurring in the pin-hole reactor with the increasing applied voltage: (a) electrolysis (frequency of 50.5 kHz), (b) bubble formation (30.2 kHz), (c) discharge operation (22.0 kHz), (d) maximal discharge operation (20.8 kHz); NaCl solution ( $500 \mu\text{S}\cdot\text{cm}^{-1}$ ), dielectric barrier thickness of 0.6 mm, pin-hole diameter of 0.6 mm.

Both high voltage amplitude as well as voltage measured on the capacitor increased with the increasing applied voltage. During the phase when only electrolytic reactions proceed in the reactor (no sound or light records were observed), high voltage between electrodes oscillated up to 300 V. When the applied voltage amplitude was increased up to 800 V, the first bubbles appeared in the pin-hole vicinity due to the solution heating and evaporation. Discharge breakdown in the pin-hole was observable when high voltage reached amplitudes over 1000 V. Maximal source operation gave the amplitude around 4000 V. Simultaneously with the increasing applied voltage, discharge frequency decreased in the audio range. In order to evaluate discharge power, an integral area ( $A$ ) of the curve in each Lissajouse chart was calculated. Subsequently, discharge power was calculated according to the following equation:

$$P = A \cdot C \cdot f \quad (1)$$

where  $A$  is the integral area of the curve ( $V^2$ ),  $C$  is capacitance of the capacitor ( $4.142 \mu\text{F}$ ) and  $f$  is adjusted frequency (Hz).

The values of discharge power were evaluated as a function of the high voltage amplitude (Figure 3 left) or frequency (Figure 3 right). Presented data were obtained in NaCl solution (conductivity of  $500 \mu\text{S}\cdot\text{cm}^{-1}$ ) and with the ceramic barrier (thickness of 0.6 mm) in which the discharge was created in one central pin-hole with a 0.6 mm diameter. Figure 3 left represents an example of the discharge generation characteristic. The initial part (I) shows a very slow increase of energy dissipated in the system on applied voltage, and it corresponds to ohmic character of the interelectrode system. This means that there is no discharge created and only electrolytic reactions can proceed in the system. The second part (II) is characterized by a significantly higher power consumption which corresponds to the bubbles formation. Presence of bubbles was also confirmed visually, and significant sound generation caused by their cavitation was recorded. Finally, the third part (III) represents the discharge operation. A chaotic character of experimental points reflects the fact that the discharge is not operating continuously. It is generated inside the bubbles that cavitate and thus the power consumption is strongly dependent on the bubbles dimensions, mainly. Transitions between these determined parts expressed by the applied high voltage magnitude are as follows: 500 V for the start of bubble formation and 900 V for the discharge breakdown.

Dependence of discharge power on applied frequency is shown in Figure 3 right. Discharge power more or less exponentially decreases with the increasing frequency in the audio range (20–72 kHz) from 44 to less than 1 W.

To compare plasma creation at different pin-hole conditions, results obtained with the ceramic barrier in which one central pin-hole with a 0.3 mm diameter are presented in Figure 4. The discharge characteristic (Figure 4 left) shows that the transitions between the observed processes are different for the smaller pin-hole diameter: 900 V for the bubble formation and over 2300 V for the discharge breakdown. On the other hand, dependence of discharge power on applied frequency seems to be similar for both pin-hole diameters (Figure 4 right).

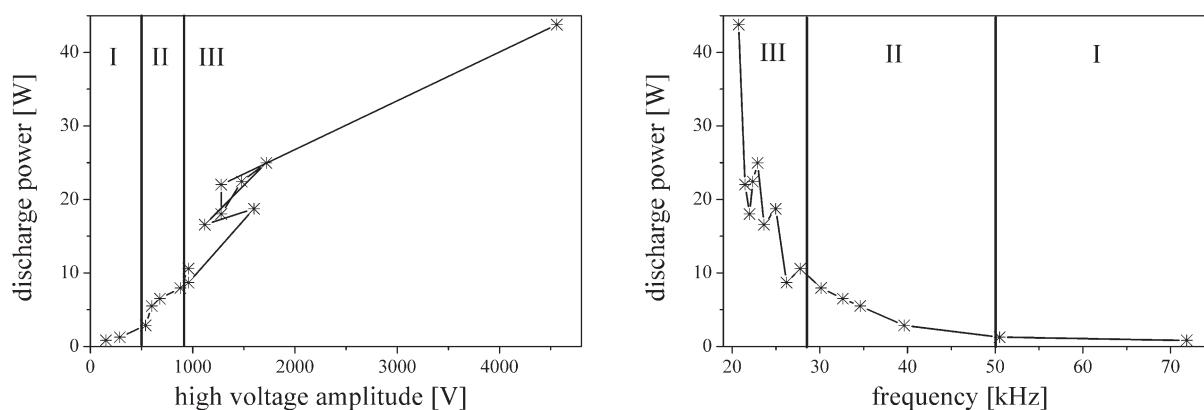


Figure 3. Dependence of discharge power on applied high voltage amplitude (left) and frequency (right); NaCl solution ( $500 \mu\text{S}\cdot\text{cm}^{-1}$ ), dielectric barrier thickness of 0.6 mm, pin-hole diameter of 0.6 mm. I – electrolysis, II – bubble formation, III – regular discharge operation.

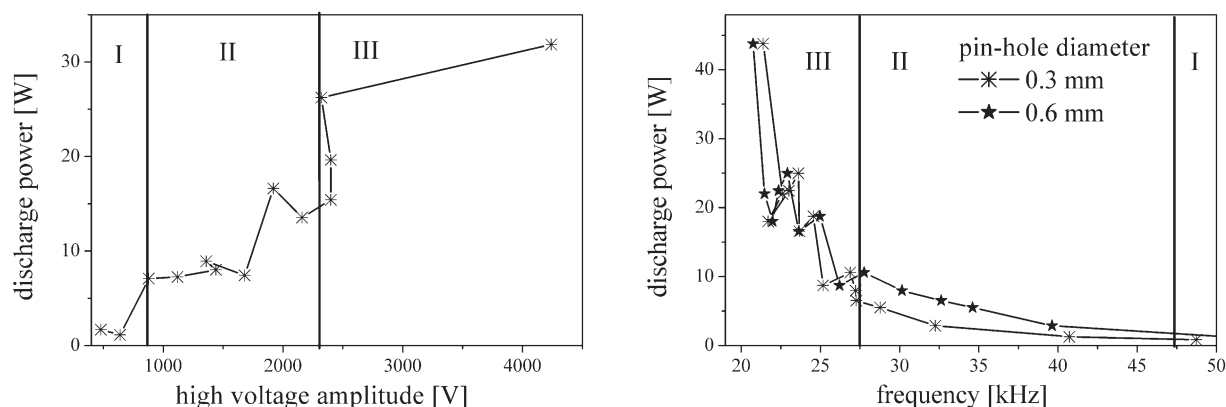


Figure 4. Left: Dependence of discharge power on applied high voltage amplitude for 0.3 mm pin-hole diameter. Right: Comparison of discharge power as a function of applied frequency for different pin-hole diameters. Both: NaCl solution ( $500 \mu\text{S}\cdot\text{cm}^{-1}$ ), dielectric barrier thickness of 0.6 mm.

## Conclusions

The paper describes ignition of the pin-hole discharge generated by high frequency high voltage in NaCl solution. Based on electric measurements of discharge current and voltage as well as sound and light records, three phases during the discharge generation were determined. Discharge energy was calculated by Lissajouse charts for each phase. Subsequently, discharge power was estimated and evaluated as a function of applied high voltage amplitude and frequency. Results were compared for two pin-hole diameters. While the dependence of discharge power on applied frequency seems to be independent on the pin-hole diameter, discharge characteristics (i.e. dependence of discharge power on high voltage amplitude) are different as well as appearance of observed processes. Both bubble formation and discharge breakdown starts at substantially higher applied voltage in the case of smaller pin-hole diameter. This fact is caused by a relatively higher resistance of the system with the smaller pin-hole diameter.

## Acknowledgements

This work was supported by the Czech Ministry of Culture, project No. DF1101OVV004.

## References

- [1] Kozáková Z., Nejezchleb M., Krčma F., Halamová I., Čáslavský J., Dolinová J., “Removal of Organic Dye Direct Red 79 from Water Solutions by DC Diaphragm Discharge: Analysis of Decomposition Products”, *Desalination*, 258, pp. 93-99, 2010
- [2] A.T. Sugiarto, S. Ito, T. Ohshima, M. Sato, J.D. Skalný, “Oxidative decoloration of dyes by pulsed discharge in water”, *J. Electrostatics*, 58, pp. 135-145, 2003
- [3] L. Marsili, S. Espie, J.G. Anderson, S.J. MacGregor, “Plasma inactivation of food-related microorganisms in liquids”, *Radiat. Phys. Chem.*, 65, pp. 507-513, 2002
- [4] M. Klíma, P. Slavíček, M. Šíra, T. Čižmár, P. Vaněk, “HF plasma pencil and DC diaphragm discharge in liquids diagnostics and applications”, *Czech. J. Phys.*, 56, pp. B1051-B1056, 2006
- [5] S.M. Thagard, K. Takashima, A. Mizuno, “Electrical discharges in polar organic liquids”, *Plasma Process. Polym.*, 6, pp. 741-750, 2009
- [6] *Plasma Chemistry and Catalysis in Gases and Liquids*, eds. V.I. Parvulescu, M. Magureanu, P. Lukes, Wiley-VCH, 2012
- [7] Z. Stará, F. Krčma, “Degradation of Organic Dyes Versus  $\text{H}_2\text{O}_2$  Generation During the DC Diaphragm Discharge Treatment in Water Solutions”, *Acta Physica Slovaca*, 55, pp. 515-519, 2005
- [8] H.E. Wagner, R. Brandenburg, K.V. Kozlov, A. Sonnenfeld, P. Michel, J.F. Behnke, “The barrier discharge: basic properties and applications to surface treatment”, *Vacuum*, 71, pp. 417-436, 2003